American Mineralogist, Volume 72, pages 468–480, 1987

Ternary-spinel volumes in the system $MgAl_2O_4$-Fe_3O_4-$\gamma Fe_{8/3}O_4$: Implications for the effect of *P* on intrinsic f_{O_2} measurements of mantle-xenolith spinels

GLEN S. MATTIOLI,* BERNARD J. WOOD
Department of Geological Sciences, Northwestern University, Evanston, Illinois 60201, U.S.A.
IAN S. E. CARMICHAEL
Department of Geology and Geophysics, University of California at Berkeley, Berkeley, California 94720, U.S.A.

ABSTRACT

Volume-composition relations along the $MgAl_2O_4$-Fe_3O_4 spinel join were determined as a function of f_{O_2}, defect concentration, and temperature of synthesis. The partial molar volumes of Fe_3O_4 and $\gamma Fe_{8/3}O_4$ components in synthetic spinels were measured by X-ray powder diffraction, and a volume model for $MgAl_2O_4$-Fe_3O_4-$\gamma Fe_{8/3}O_4$ ternary spinels was derived from our data and those summarized by Lindsley (1976) for the Fe_3O_4-$\gamma Fe_{8/3}O_4$ spinel join. Least-squares fits to the binary and ternary data resulted in linear volume-composition relations for the Fe_3O_4-$\gamma Fe_{8/3}O_4$ and $MgAl_2O_4$-$\gamma Fe_{8/3}O_4$ spinel joins. The $MgAl_2O_4$-Fe_3O_4 join, however, shows a significant positive deviation from ideality, and the following asymmetric thermodynamic parameters and their associated uncertainties were derived: $V^0_{mt} = 1.066 \pm 0.014$, $V^0_{sp} = 0.950 \pm 0.001$, $W^V_{mt\text{-}sp} = 0.043 \pm 0.012$, and $W^V_{sp\text{-}mt} = 0.018 \pm 0.004$, all in cal/bar.

The volume data were used to estimate the effect of pressure on published intrinsic f_{O_2} measurements of mantle spinels and to correct polyphase thermobarometric f_{O_2} estimates to upper-mantle pressures. We find that 1-atm intrinsic and thermobarometric f_{O_2} estimates change less than 1 log unit relative to the synthetic Fe buffers at 15-kbar total pressure, which suggests that a mechanism other than pressure is responsible for producing the apparently highly reducing f_{O_2} values determined by the intrinsic method.

The observed cell-edge data for the $MgAl_2O_4$-Fe_3O_4 join were also compared to predicted cell edges based on cation distributions calculated between 500 and 1400°C using the O'Neill and Navrotsky (1983, 1984) model. We have found that their model does not exactly reproduce cell edge–composition relations along this join, probably because of varying extents of re-equilibration during the quench from high temperature.

INTRODUCTION

Spinels have wide geologic distribution as accessory minerals in crustal igneous and metamorphic rocks and as the characteristic phase of the spinel lherzolite facies of the Earth's upper mantle. Furthermore, naturally occurring spinels are typically compositionally complex and have equilibrated under a wide range of temperature and pressure conditions. This compositional variation makes them useful indicators of petrologic conditions of formation (Sack, 1982), if the component chemical potentials are known as functions of temperature, pressure, and bulk composition. In particular, because oxide spinels are stable over a considerable pressure range (1 atm to 40 kbar, for Cr-rich spinel), precise volume-composition data are needed to calculate the effect of pressure on thermobarometric equilibria involving a spinel phase (e.g., Buddington and Lindsley, 1964; Gasparik and Newton, 1984). In addition to their petrologic utility, volume-composition data may be used as a test of O'Neill and Navrotsky's (1983, 1984) model of cation distribution in spinel, which predicts macroscopic thermodynamic properties (molar volumes, component activities, consolute temperatures) from the energetics of microscopic phenomena.

In this paper, we present volume-composition data for the pseudobinary-spinel join $MgAl_2O_4$-Fe_3O_4 as a function of f_{O_2}, defect concentration, and temperature. The thermodynamics of this pseudobinary are important because mantle-derived spinels are rich in $MgAl_2O_4$ component and their Fe_3O_4 component exerts a major control on their magnetic, electronic, and transport properties. In addition, Fe_3O_4 is the main Fe^{3+} component in the spinel lherzolite facies, and hence its concentration may be used to estimate the equilibrium f_{O_2} recorded by spinel-bearing, mantle-derived xenoliths (Mattioli and Wood, 1986a, 1987). X-ray powder-diffraction measurements of unit-cell edges across the $MgAl_2O_4$-Fe_3O_4 spinel join, in con-

---

* Current address: Division of Geological and Planetary Sciences, California Institute of Technology, Pasadena, California 91125, U.S.A.

0003–004X/87/0506–0468$02.00

cert with wet-chemical analyses of Fe^{2+}/Fe^{3+} ratios of synthetic spinels equilibrated at known f_{O_2}, allow calculation of the partial molar volumes of both Fe_3O_4 and $\gamma Fe_{8/3}O_4$ components in $MgAl_2O_4$-rich spinels. These results, when combined with published data for the Fe_3O_4-$\gamma Fe_{8/3}O_4$ join (Lindsley, 1976), define partial molar volumes within the $MgAl_2O_4$-Fe_3O_4-$\gamma Fe_{8/3}O_4$ ternary-spinel system.

Immediate applications of the volume data are (1) to correct thermobarometric estimates of upper-mantle f_{O_2} based on coexisting spinel-orthopyroxene-olivine assemblages to mantle pressures (Mattioli and Wood, 1986a), and (2) to determine whether pressure is important in producing the apparently low f_{O_2} values measured by 1-atm intrinsic studies of mantle xenoliths (Arculus and Delano, 1980, 1981; Arculus et al., 1984). This effect may be evaluated by determining the pressure dependence of concentration of defect spinel ($\gamma Fe_{8/3}O_4$) at fixed temperature, f_{O_2}, and Fe/$MgAl_2O_4$ ratio. Finally, the data provide a test of the O'Neill-Navrotsky cation-distribution model as applied to complex spinel systems.

SPINEL STRUCTURE AND CATION DISTRIBUTION

A cubic closest-packed array of oxygen anions, with metal cations occupying ⅛ of the available tetrahedral and ½ of the octahedral interstices, defines the spinel crystallographic structure (Hill et al., 1979). Three parameters are necessary to describe the spinel structure: (1) the unit-cell edge, a (in Å), which is used to calculate molar volumes; (2) the oxygen parameter, u, which measures the deviation from an ideal cubic closest-packed lattice; and (3) a stoichiometry parameter, δ, which measures the deviation from 3 cations per 4 oxygens. An ideal, defect-free spinel has a cation to oxygen ratio of 3:4 and crystallizes in the space group $Fd3m$.

Despite the fact that spinels occur in a wide variety of igneous and metamorphic assemblages, nearly 98% of the cations found in natural spinels are in the set $\{Mg^{2+}, Fe^{2+}, Al^{3+}, Cr^{3+}, Fe^{3+}, Ti^{4+}\}$ (Sack, 1982). These cations reside on both tetrahedral and octahedral sublattices, and unary, i.e., single-component, spinels show temperature-dependent order-disorder relations (Wu and Mason, 1981; Wood et al., 1986; Navrotsky and Kleppa, 1967), such that the cation distribution of 2–3 spinels, for example, varies between ideal $A^{2+}(B^{3+})_2O_4$ "normal" and $B^{3+}(A^{2+},B^{3+})O_4$ "inverse" limits, where the species in parentheses reside on octahedral sites. $MgAl_2O_4$ (spinel, sensu stricto) is dominantly "normal" at temperatures below 600°C and becomes increasingly inverted at higher temperatures (Wood et al., 1986; Navrotsky, 1986), whereas Fe_3O_4 (magnetite) is dominantly "inverse" at low temperatures and has a nearly random cation distribution at 1450°C (Wu and Mason, 1981). The cation distribution in complex binary-spinel solid solutions may be either temperature (Navrotsky and Kleppa, 1967) or composition (Trestman-Matts et al., 1984; Mason, 1985) dependent or both (Trestman-Matts et al., 1983; Mattioli and Wood, 1986b; Hill and Sack, 1987). If the cation and anion radii for all the substituting species in both octahedral and tetrahedral coordination (Shannon and Prewitt, 1969; Shannon, 1976) and values of the O'Neill-Navrotsky parameters, α and β, are known, then the equilibrium cation distribution, cell edge, and molar volume for a binary spinel may be calculated as a function of composition and temperature. The generated volume-composition relations may then be compared to observed cell edges, to test both the model parameters and the applicability of a microscopic formulation of macroscopic properties. This test is important for the $MgAl_2O_4$-Fe_3O_4 spinel join because the end members have different cation distributions at low temperature and because there are no available experimental data that explicitly constrain the ordering state of intermediate-spinel solid solutions.

EXPERIMENTAL AND ANALYTICAL PROCEDURES

Synthesis methods

Analytical-grade aluminum hydroxide and magnesium carbonate were dehydrated and decarbonated at 800 and 1300°C and 1-atm pressure in air, respectively, to produce Al_2O_3 and MgO. Adsorption of H_2O onto MgO powder is significant during cooling from 1300°C in air, and this effect was measured by weighing the MgO at fixed intervals until a stable value was achieved. The dried Al_2O_3 and MgO powders were weighed in stoichiometric proportions to yield $MgAl_2O_4$ and ground together under reagent-grade acetone with a few drops of butyl acetate (Duco cement) added as a binder. The resultant mix was pressed into a pellet and dried at 120°C overnight, then held at 800°C for 48 h, and finally sintered on Pt foil at 1400°C for 48 h, with all synthesis steps completed in air at 1-atm total pressure. A small amount (approximately 1 to 2 wt%) of unreacted MgO was detected by X-ray diffraction after the initial 48 h at 1400°C. The spinel was reground and repressed, and the procedure outlined above was repeated. This produced a well-crystallized and homogeneous spinel (with no detectable unreacted oxides), which later was used as a starting material in syntheses of $MgAl_2O_4$-Fe_3O_4 solid solutions.

Magnetite was synthesized by mixing analytical-grade anhydrous Fe_2O_3 and Fe metal in a molar ratio of 0.95:1.10. The mix was sealed in annealed Au capsules with a few drops of H_2O added as a flux. The Au capsules were held at 800°C and 1 kbar in standard cold-seal vessels for 24 h and were then quenched rapidly at constant pressure. Pure Fe_3O_4 was produced. Defect-rich magnetitie was synthesized from sintered hematite at 1500°C in air.

$MgAl_2O_4$-Fe_3O_4 solid solutions were synthesized either by mixing MgO, Al_2O_3, and Fe_2O_3 or $MgAl_2O_4$ and Fe_3O_4 in stoichiometric proportions, pressing the mixes into pellets, and then sintering on Pt foil at 1400 to 1500°C in air for two cycles, to produce well-crystallized and homogeneous spinel solid solutions (as indicated by sharpness and splitting of the X-ray peaks). The spinels were generally quenched in H_2O to help retain their high-temperature defect concentrations and cation distributions. Spinels synthesized in air at 1400 to 1500°C by these methods crystallize in the $MgAl_2O_4$-Fe_3O_4-$\gamma Fe_{8/3}O_4$ ternary system; however, defect concentrations increase exponentially toward the Fe_3O_4-rich end of the $MgAl_2O_4$-Fe_3O_4 join, so $MgAl_2O_4$-rich spinels are close to stoichiometric when synthesized in air at high temperature ($\geq$1400°C) (Dieckmann, 1982). Defect spinels were re-equilibrated at 1400°C in a 100 ppm O_2 (balance, Ar) gas stream for 2 h and were then quenched to 25°C in H_2O to produce stoi-

TABLE 1. Synthesis conditions and average cell-edge and molar-volume data

Sample*	T (°C)	f_{O_2} (atm)	s. m.**	Duration (h)	$X_{Fe_3O_4}$	a (Å)	V (cm³)
114A	1400	0.21	A	48	0.00	8.0855(11)	39.790(13)
114D	1000	"oxidized"	A	5	0.00	8.0857(12)	39.793(14)
115A	1400	0.21	A	48	0.02	8.0934(7)	39.907(8)
115C	1000	10^{-8}	A	5	0.02	8.0943(5)	39.920(6)
115E	1000	1.0% CO	A	5	0.02	8.0950(8)	39.930(10)
111A	1400	0.21	A	48	0.05	8.1047(8)	40.074(10)
111C	1000	10^{-8}	A	5	0.05	8.1053(8)	40.083(10)
111E	1000	1.0% CO	A	5	0.05	8.1079(12)	40.122(14)
161A	1450	0.21	B	48	0.05	8.1073(8)	40.113(10)
132A	1400	0.21	A	48	0.08	8.1180(8)	40.272(10)
132C	1000	10^{-8}	A	5	0.08	8.1167(10)	40.252(12)
132E	1000	1.0% CO	A	5	0.08	8.1204(10)	40.308(12)
112A	1400	0.21	A	48	0.10	8.1254(5)	40.382(6)
112C	1000	10^{-8}	A	5	0.10	8.1236(12)	40.355(14)
112E	1000	1.0% CO	A	5	0.10	8.1286(12)	40.430(14)
156A	1450	0.21	B	60	0.10	8.1254(11)	40.382(13)
156B	1400	10^{-4}	A	2	0.10	8.1231(10)	40.348(12)
182A	1450	0.21	B	60	0.10	8.1244(10)	40.367(12)
182B	1400	10^{-4}	B	2	0.10	8.1231(8)	40.348(10)
128A	1400	0.21	A	48	0.20	8.1596(7)	40.894(8)
128C	1000	10^{-8}	A	5	0.20	8.1603(11)	40.905(13)
128E	1000	1.0% CO	A	5	0.20	8.1661(11)	40.992(13)
133A	1400	0.21	B	48	0.33	8.2013(9)	41.524(11)
133E	1000	1.0% CO	B	5	0.33	8.2098(14)	41.654(17)
133D	1000	"oxidized"	B	5	0.33	8.1805(16)	41.209(19)
181A	1450	0.21	B	60	0.35	8.2106(9)	41.666(11)
181B	1400	10^{-4}	B	2	0.35	8.2183(9)	41.783(11)
135A	1400	0.21	B	48	0.43	8.2321(11)	41.994(13)
135D	1000	"oxidized"	B	5	0.43	8.2007(8)	41.515(10)
160A	1450	0.21	B	48	0.45	8.2408(10)	42.127(12)
160B	1400	10^{-4}	B	2	0.45	8.2490(11)	42.253(13)
137A	1450	0.21	B	48	0.53	8.2640(13)	42.484(16)
137D	1000	"oxidized"	B	5	0.53	8.2292(18)	41.950(22)
157A	1450	0.21	B	48	0.55	8.2672(16)	42.533(19)
157B	1400	10^{-4}	B	2	0.55	8.2787(12)	42.711(14)
138A	1450	0.21	B	48	0.63	8.2905(9)	42.894(11)
138D	1000	"oxidized"	B	5	0.63	8.2601(14)	42.424(17)
141A	1450	0.21	B	48	0.72	8.3164(14)	43.297(17)
159A	1450	0.21	B	48	0.75	8.3228(12)	43.397(14)
159B	1400	10^{-4}	B	2	0.75	8.3330(16)	43.557(19)
180A	1450	0.21	B	48	0.75	8.3223(6)	43.389(7)
180B	1400	10^{-4}	B	2	0.75	8.3332(7)	43.560(8)
142A	1450	0.21	B	48	0.82	8.3404(18)	43.673(22)
142D	1000	"oxidized"	B	5	0.82	8.3306(24)	43.519(29)
158A	1450	0.21	B	48	0.85	8.3463(25)	43.766(30)
158B	1400	10^{-4}	B	2	0.85	8.3584(15)	43.956(18)
179A	1450	0.21	B	48	0.85	8.3447(18)	43.741(22)
179B	1400	10^{-4}	B	2	0.85	8.3587(8)	43.961(10)
178A	1450	0.21	B	48	0.92	8.3656(9)	44.070(11)
178B	1400	10^{-4}	B	2	0.92	8.3760(8)	44.235(10)
173A	1500	0.21	B	48	1.00	8.3924(15)	44.495(18)
173B	1400	10^{-4}	B	2	1.00	8.3956(8)	44.546(10)
175A	1500	0.21	B	48	1.00	8.3923(9)	44.494(11)
175B	1400	10^{-4}	B	2	1.00	8.3989(5)	44.599(6)
125F	800; 1 kbar	~NNO	C	24	1.00	8.3980(9)	44.584(11)
127F	800; 1 kbar	~NNO	C	24	1.00	8.3967(22)	44.564(25)
130F	800; 1 kbar	~NNO	C	24	1.00	8.3992(19)	44.603(22)
145F	800; 1 kbar	~NNO	C	24	1.00	8.3977(10)	44.580(12)

Note: Values in parentheses are $\pm 1\sigma$ for the final decimal place.

* Letter codes are the same in Table 2.

** Starting mixture: A = MgO, Al_2O_3, and Fe_2O_3; B = $MgAl_2O_4$ and Fe_3O_4; C = Fe and Fe_2O_3.

chiometric-spinel solid solutions. In addition, some spinels of intermediate composition were re-equilibrated at 1000°C in a CO-CO_2 gas mix with an apparent f_{O_2} of 10^{-8} atm. During the syntheses, the f_{O_2} was monitored by a Ceramic Oxide Fabricators, Inc., yttria-stabilized zirconia solid electrolyte (Sato, 1971) and was in agreement to within ±0.10 log units of the f_{O_2} calculated from the tables of Deines et al. (1974) for the appropriate gas mixture. The spinels were cooled to 500°C at f_{O_2} values below QFM and then removed from the furnace. This procedure produced relatively defect-poor spinels at low total Fe content ($X_{Fe_3O_4} \leq 0.35$) and reddish-colored, oxidized-looking, defect-rich spinels at high total Fe content ($X_{Fe_3O_4} \geq 0.35$). We ascribe the defect-rich products to disequilibrium of the furnace's gases at low temperature, and we therefore denote these samples as "oxidized" in Table 1. In addition, some spinels with $X_{Fe_3O_4} \leq 0.35$ were equilibrated in an unbuffered but reducing atmosphere of

1.0% CO (balance, Ar). The synthesis conditions for each composition are presented in Table 1.

Representative samples in the composition range 0.05 to 0.85 mole fraction Fe_3O_4 were selected from the five different f_{O_2} conditions (0.21, 10^{-4} atm, 10^{-8} atm, "oxidized," and 1.0% CO) for wet-chemical determination of FeO content. Concentrated HF was used to dissolve approximately 1 to 2 mg of synthetic spinel prior to analysis. The actual FeO content was determined by the ammonium metavanadate titration method of Wilson (1960), and the total Fe content (FeO_t) was verified by electron microprobe, as discussed below. Actual FeO analyses are reproducible to within ±0.5 wt%. Results are presented in Table 2 and discussed further below.

Unit-cell refinements

Unit-cell edges of synthetic spinels across the $MgAl_2O_4$-Fe_3O_4 join were measured for the five different f_{O_2} conditions. Slow-scan (¼° 2θ/min) X-ray diffractograms were collected by scanning both in the increasing and decreasing 2θ directions from 47° to 67° 2θ. The 220 and 311 reflections of an internal Si-metal standard were used to calibrate the position of spinel 422, 511, and 440 reflections generated by Cu$K\alpha_1$ radiation ($\lambda = 1.5405$ Å). For some unit-cell determinations, only 422 and 511 spinel reflections and 311 Si-metal reflection were indexed. All X-ray diffraction patterns used for unit-cell refinements showed good Cu$K\alpha_1$-Cu$K\alpha_2$ splitting and sharp standard and spinel reflections of appropriate intensity. Each spinel peak was used to calculate a unit-cell edge; normally, a total of 12 or more peaks was indexed, and the 422, 511, and 440 reflections were averaged together and separately to calculate sample means and standard deviations. No difference, within $\pm 1\sigma$, was observed either among mean unit-cell edges for individual reflections or between individual means and the mean unit-cell edge based on all 12 or more peaks, which suggests that no systematic bias is present in the calibration of unknown peaks with respect to standard peaks. Unit-cell edges for each composition have sample means with standard deviations of approximately 10^{-3} Å. In addition, repeat syntheses of spinels of fixed composition at the same T, f_{O_2} conditions yielded sample means of unit-cell edges that are within $\pm 1\sigma$, suggesting that accuracy and precision of cell-edge measurement are of the same order of magnitude. Average cell edges and calculated molar volumes are presented together with synthesis conditions in Table 1.

Electron-microprobe analyses

In addition to wet-chemical analysis and X-ray diffraction, spinel solid solutions were checked for homogeneity and stoichiometry by electron microprobe. Selected samples in the composition range 0.05 to 0.92 mole fraction Fe_3O_4 were mounted and polished. The small grain size of the synthetic spinels made polishing difficult, although for most samples small areas (about 400 μm^2) did polish well enough for microprobe analysis. The analyses were conducted on the JEOL 733 Superprobe in the Department of Geological Sciences at Northwestern University. Operating conditions were 15-kV accelerating potential, 30-nA Faraday cup current, and a beam-spot diameter of approximately 1 μm. A natural chromite (USNM 117075) from the Tiebaghi Mine, New Caledonia, was used as a standard for Mg, Al, and Fe. Characteristic $K\alpha$ lines were used for wavelength-dispersive analysis of all three elements, with Mg and Al X-rays and Fe X-rays collected with individual TAP and LIF crystals, respectively. Raw count data were corrected and reduced following the procedures of Bence and Albee (1968) and Albee and Ray (1970).

The chromite standard was treated as an unknown before and after each analytical session, which normally lasted between 6 and 8 h. Automated line scans, with individual spot analyses about 2 to 5 μm apart, were conducted across the sample. Up to 30 analyses were collected and averaged, and within the analytical uncertainty arising from counting statistics alone (approximately 1 to 2% relative), no difference between the mean observed and reported concentration of the three elements was apparent either before and after each session or among probe sessions. Synthetic-spinel solid solutions also were analyzed using an automated line-scan routine. Normally, two to six line scans were completed to test for element zoning and to identify any non-spinel phases, which might have escaped detection by X-ray diffraction. Up to 39 analyses for each composition were collected and averaged. The synthetic spinels were not zoned, and no evidence of additional phases was found. In fact, the observed compositions and Fe^{2+}/Fe^{3+} ratios calculated by stoichiometry from the microprobe data are within 2 mol% of the nominal values for spinels reequilibrated at 1400°C and an f_{O_2} of 10^{-4} atm, whereas those reequilibrated under oxidizing conditions apparently are defect ($\gamma Fe_{8/3}O_4$) rich. Complete results are presented in Table 3.

TABLE 2. Wet-chemical analyses of synthetic spinels

Sample*	$X_{MgAl_2O_4}$	FeO_{act} (wt%)	$X_{Fe_3O_4}$	$X_{\gamma Fe8/3O4}$	$X_{Fe_4O_4}$
111A	0.95	1.02	0.02	0.03	—
111E	0.95	3.92	0.02	—	0.03
132A	0.92	1.76	0.04	0.04	—
132C	0.92	1.20	0.03	0.05	—
132E	0.92	4.45	0.07	—	0.01
112A	0.90	1.87	0.04	0.06	—
112E	0.90	6.94	0.06	—	0.04
156A	0.90	1.89	0.04	0.06	—
156B	0.90	5.26	0.09	—	0.01
128A	0.80	5.04	0.12	0.08	—
128E	0.80	14.61	0.18	—	0.02
133A	0.67	10.67	0.28	0.05	—
133E**	0.67	29.30	0.15	—	0.18
135A	0.57	13.96	0.38	0.05	—
135D	0.57	1.98	0.08	0.35	—
160A	0.55	8.26	0.28	0.17	—
160B	0.55	17.12	0.44	0.01	—
157A	0.45	13.98	0.45	0.10	—
157B	0.45	18.14	0.52	0.03	—
138A	0.37	18.06	0.57	0.06	—
138D	0.37	3.84	0.22	0.41	—
159A	0.25	19.06	0.69	0.06	—
159B	0.25	25.21	0.75	—	—
158A	0.15	21.17	0.81	0.04	—
158B	0.15	26.72	0.84	0.01	—

* See Table 1 for synthesis conditions.

** Possible grain-boundary film of metallic Fe interfering with chemical analysis.

RESULTS

Least-squares regression

Least-squares polynomial fits of the cell edge–composition data were completed for the various T, f_{O_2} conditions (Table 1). Molar volumes were calculated from the raw cell-edge data, and volume-composition data were also fit using the method outlined below. The polynomial is of the form

$$f(X) = \alpha_0 X^0 + \alpha_1 X^1 + \alpha_2 X^2 + \alpha_3 X^3 + \ldots + \alpha_n X^n, \quad (1)$$

where $f(X)$ is cell edge or molar volume, X is the nominal mole fraction of Fe_3O_4, and α_0 to α_n are the fit coefficients.

TABLE 3. Average electron-microprobe analyses of synthetic spinels

Run:	111A	112A	182B	128A	133E	181B	135E	180B	179B	178B
Nominal $X_{Fe_2O_4}$:	0.05*	0.10	0.10	0.20	0.33	0.35	0.43	0.75	0.85	0.92
N:	10	28	21	38	25	29	18	39	27	25
MgO (wt%)	26.84(0.76)	24.02(0.37)	24.37(0.65)	20.52(0.38)	15.88(0.52)	15.45(0.17)	12.64(0.93)	5.03(0.07)	2.91(0.04)	1.60(0.02)
Al_2O_3 (wt%)	61.01(1.13)	55.81(0.57)	61.10(0.86)	47.93(0.75)	37.92(0.35)	38.80(0.25)	32.99(1.34)	12.38(0.21)	7.29(0.08)	3.99(0.03)
FeO_t (wt%)	7.62(0.23)	14.71(0.38)	14.73(0.27)	27.33(0.47)	42.55(0.98)	44.95(0.47)	52.23(2.38)	77.91(0.40)	84.38(0.44)	84.75(0.66)
Total	95.56(1.70)	94.55(0.81)	100.21(1.03)	95.80(0.94)	96.34(0.81)	99.21(0.49)	97.89(1.36)	95.32(0.45)	94.63(0.36)	90.46(0.59)
Mg^{2+}	1.04(0.02)	0.98(0.01)	0.93(0.02)	0.89(0.01)	0.75(0.02)	0.71(0.01)	0.63(0.04)	0.32(0.00)	0.20(0.00)	0.12(0.00)
Al^{3+}	1.86(0.01)	1.79(0.01)	1.84(0.02)	1.63(0.01)	1.42(0.01)	1.42(0.01)	1.29(0.04)	0.62(0.00)	0.39(0.00)	0.23(0.00)
Σ Fe	0.17(0.01)	0.34(0.01)	0.31(0.01)	0.66(0.01)	1.13(0.02)	1.16(0.01)	1.45(0.08)	2.76(0.01)	3.21(0.01)	3.53(0.00)
Mg/Al**	0.56	0.54	0.50	0.54	0.53	0.50	0.49	0.52	0.50	0.51
$X^{calc}_{Fe_3O_4}$**	0.00	0.06	0.10	0.16	0.32	0.35	0.43	0.74	0.84	0.91
$X^{calc}_{\gamma Fe_{8/3}O_4}$**	0.06	0.06	0.01	0.05	0.03	0.00	0.00	0.01	0.00	0.00

Note: Values in parentheses are ±1σ.
* Extremely poor polish on sample.
** Based on an ideal formula of 3 cations per 4 oxygens.

Sample means were weighted by reciprocal variance. FORTRAN computer programs used to fit the data were taken and modified from Bevington (1969). The numerical method reduces the sum of the squares of the residuals of a given set of data and their associated standard deviations for a polynomial of specified order (n). The fitting procedure assumes that there is no uncertainty in the independent variable, in this case, $X_{Fe_3O_4}$.

Additional parameters (n) always will improve the goodness of fit to any particular number of data points (N). A "perfect" fit is achieved when $N = n - 1$, and the degree of freedom goes to zero; however, these additional fit parameters may not be statistically significant at a reasonable confidence level for the number and quality of the experimental data. The statistical F-test may be used to evaluate whether an additional parameter should be included in the fitting polynomial. The F-ratio is defined as

$$F_x = \frac{\Delta\chi^2}{\chi^2_\nu} \qquad (2)$$

where $\Delta\chi^2$ is the difference in chi-squared between a fit with $(n - 1)$ and (n) parameters, and χ^2_ν is the reduced chi-squared for (n) parameters (Bevington, 1969, p. 200). If the additional parameter is statistically significant, then the F_x value should be large. In addition, the calculated F_x value may be compared with tabulated F values computed for different probabilities (e.g., 99% and 95%) for a numerator degree of freedom of 1. All polynomial fits presented here were truncated when the F_x value fell below the F value calculated for the 95% confidence level. More sophisticated statistical tests may be applied to determine whether or not additional terms are merited in least-squares polynomial fits (see, e.g., Powell, 1985). Because the current data are free of "outliers," however, we feel that such treatment is unnecessary for the purposes of this study. The values of the derived fit coefficients, their associated standard errors, and F_x are presented in Table 4. The standard thermodynamic parameters V^0_1, V^0_2, W^V_{12}, and W^V_{21} are related to the coefficients α_0 to α_3 as follows:

—polynomial of order 2: symmetric binary—

$$V^0_1 = \alpha_0 + \alpha_1 + \alpha_2$$
$$V^0_2 = \alpha_0$$
$$W^V_{12} = W^V_{21} = -\alpha_2$$

—polynomial of order 3: asymmetric binary—

$$V^0_1 = \alpha_0 + \alpha_1 + \alpha_2 + \alpha_3$$
$$V^0_2 = \alpha_0$$
$$W^V_{12} = -\alpha_3 - \alpha_2$$
$$W^V_{21} = -\alpha_2 - 2\alpha_3,$$

where subscript 1 = Fe_3O_4 and subscript 2 = $MgAl_2O_4$. In Table 5 we present an example of a correlation matrix for the least-squares fit to the syntheses at 1400°C and 10^{-4} atm (see discussion below).

TABLE 4. Binary cell-edge and molar-volume fit parameters

Conditions*	N	Cell edge (Å) α_0	α_1	α_2	α_3	F_x	Volume (cal/bar) α_0	α_1	α_2	α_3	F_x
A	24	8.0852	0.4152	−0.2005	0.0909	54.80	0.9509	0.1473	−0.0672	0.0318	47.92
		(0.0006)	(0.0076)	(0.0186)	(0.0123)		(0.0002)	(0.0028)	(0.0070)	(0.0046)	
B	13	8.0822	0.4465	−0.2039	0.0729	10.56	0.9498	0.1585	−0.0677	0.0249	8.87
		(0.0017)	(0.0167)	(0.0370)	(0.0224)		(0.0006)	(0.0062)	(0.0138)	(0.0084)	
C	7	8.0864	0.3830	−0.0715	—	491.78	0.9513	0.1356	−0.0214	—	346.27
		(0.0002)	(0.0033)	(0.0032)	—		(0.0001)	(0.0012)	(0.0011)	—	
D	7	8.0871	0.2332	0.0764	—	23.66	0.9516	0.0813	0.0322	—	30.62
		(0.0040)	(0.0162)	(0.0157)	—		(0.0015)	(0.0060)	(0.0058)	—	
E	8	8.0860	0.4484	−0.2496	0.1131	36.00	0.9512	0.1584	−0.0814	0.0374	32.52
		(0.0003)	(0.0058)	(0.0242)	(0.0189)		(0.0001)	(0.0020)	(0.0084)	(0.0066)	

Note: Values in parentheses are the standard error for each fit parameter.

* A = 1400–1500°C and 0.21 atm; B = 1400°C and 10^{-4} atm; C = 1000°C and 10^{-8} atm; D = 1000°C and "oxidized"; E = 1000°C and 1.0% CO.

DISCUSSION

Molar volumes calculated from the observed cell edges and corresponding polynomial fits to three of the five T, f_{O_2} data sets (1400–1500°C in air, 1400°C and 10^{-4} atm, and 1000°C and 10^{-8} atm) are presented in Figures 1 and 2; cell edges and molar volumes for defect-poor spinels equilibrated at 10^{-8} atm and 1.0% CO in Ar are not plotted, although these data are presented in Tables 1 and 4. Four of the five data sets show statistically significant positive deviations from ideal volumes of mixing. The results at 1000°C and a nominal f_{O_2} of 10^{-8} atm for high Fe_3O_4 concentrations ($X_{Fe_3O_4} \geq 0.35$) show, however, a negative deviation from ideal mixing (Fig. 2); these spinels have high $\gamma Fe_{8/3}O_4$ concentrations (see Table 2), which are not consistent with the nominal T, f_{O_2} conditions of the syntheses (Dieckmann, 1982). Hence cell-edge and molar-volume data for these spinels do not reflect an equilibrium defect concentration at the nominal f_{O_2} of re-equilibration; rather, their relatively small cell edges are a reflection of the high concentration of $\gamma Fe_{8/3}O_4$, which formed during cooling to 500°C in a CO_2-CO atmosphere. Later spinel syntheses were quenched to 25°C in H_2O or allowed to cool in a highly reducing atmosphere to minimize oxidation during the quench.

In contrast, spinels that were equilibrated at 1000°C in a reducing atmosphere of 1.0% CO in Ar are apparently cation rich, in that they contain slightly more than 3 cations per 4 oxygens (see Table 2). This is in part due to interstitial Fe^{2+} defects, which are observed in pure Fe_3O_4 at very low f_{O_2} (Dieckmann, 1982), and the effect may be enhanced by the presence of small amounts of metallic Fe as a grain-boundary film. Although we have not detected a metallic phase by X-ray or electron-microprobe techniques, the calculated mole fraction of defect Fe_4O_4 is much higher (up to 0.18) for one sample, no. 133E in Table 2, than observed in pure Fe_3O_4 (0.005), which suggests that a small amount of Fe metal (about 1%) is interfering with the wet-chemical analysis. Volume-composition relations and defect concentrations for the syntheses in 1.0% CO in Ar are thus no longer considered here.

The stoichiometry parameter, δ (defined as $Fe_{3-\delta}O_4$), is plotted versus log f_{O_2} for pure Fe_3O_4 at 900°C and 1-atm total pressure in Figure 3. This figure shows the respective f_{O_2} regions for Fe interstitial- and vacancy-defect populations. Thermogravimetric measurements between 900 and 1400°C indicate that the equilibrium f_{O_2} for defect-free Fe_3O_4 (i.e., $\delta = 0.0$) is shifted to more oxidizing values with increasing temperature, such that at 1400°C, $\delta = 0.0$ at an f_{O_2} of 10^{-4} atm (Dieckmann, 1982).

The cell edges of spinels re-equilibrated under oxidizing conditions are substantially smaller than those equilibrated in 1.0% CO. The differences, which increase with increasing Fe_3O_4 concentration, are due to excess Fe^{3+} in the spinel structure, which, in turn, is compensated by cation vacancies. Figure 4 shows a plot of cell edge, a, as a function of defect concentration, δ, for spinels of fixed Fe_3O_4 mole fraction and nominal composition $M_{3-\delta}O_4$. The decrease in cell edge with increasing δ may be formally attributed to increased solution of the $\gamma Fe_{8/3}O_4$ component. The volume data therefore provide information on the partial molar volume of the defect component in complex spinels.

The most extensive volume-composition data are for spinels re-equilibrated at 1400 to 1500°C in air and at 1400°C and an f_{O_2} of 10^{-4} atm. Under these conditions, spinels were synthesized at small composition intervals across the entire $MgAl_2O_4$-Fe_3O_4 join (see Fig. 1). Wet-chemical analyses were obtained for spinels with $0.05 \leq X_{Fe_3O_4} \leq 0.85$ synthesized under both T, f_{O_2} conditions; hence the concentrations of $\gamma Fe_{8/3}O_4$ and Fe_4O_4 are also constrained. Some spinel compositions were synthesized on separate occasions up to three times, thus allowing evaluation of the reproducibility of cell-edge and wet-

TABLE 5. Correlation matrix for volume fit parameters

	Volume fit for condition B* α_0	α_1	α_2	α_3
α_0	1.000	−0.794	0.674	−0.601
α_1	0.000	1.000	−0.971	0.924
α_2	0.000	0.000	1.000	−0.988
α_3	0.000	0.000	0.000	1.000

* See Table 4.

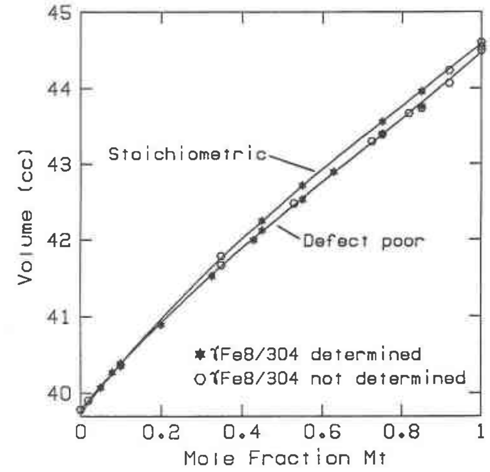

Fig. 1. Molar volumes of synthetic spinels across the Mg-Al_2O_4-Fe_3O_4 join. Data labeled stoichiometric are for spinels re-equilibrated at 1400°C and 10^{-4} atm. Data labeled defect-poor are for spinels synthesized between 1400 and 1500°C in air (see Table 1). Filled star symbols correspond to spinels that had their Fe^{2+} content measured by wet-chemical methods (see Table 2). Open hexagons correspond to spinels that did not have their Fe^{2+} content measured.The lines are least-squares fits to the plotted data (see Table 4 for fit parameters). The size of the symbols is approximately equal to $\pm 1\sigma$.

chemical measurements. All repeated syntheses yielded cell edges and defect concentrations that are identical within measurement uncertainty. Several spinels of intermediate composition were synthesized at both 1400 and 1450°C in air with similar results. For example, spinels with $X_{Fe_3O_4}$ = 0.10 (see nos. 156 and 112 in Tables 1 and 2) have cell edges and $\gamma Fe_{8/3}O_4$ concentrations that are identical, which suggests that these measurements are insensitive to such a small change in temperature. Wood et al. (1986) reported that they were unable to "quench" high-temperature cation distributions in pure $MgAl_2O_4$ above 900°C. The current syntheses of complex $MgAl_2O_4$-Fe_3O_4 spinels almost certainly behaved similarly, implying that the 1400 and 1450°C samples also had their cation distribution reset during the quench to some lower-temperature value. Vacancy mobility at high temperatures is, moreover, several orders of magnitude faster than cation mobility. In pure Fe_3O_4, with an average grain size of 10-μm diameter, vacancies would re-equilibrate in about 10^{-3} s at 1400°C (Dieckmann and Schmalzried, 1982). Spinels equilibrated at 1400°C and an f_{O_2} of 10^{-4} atm, nevertheless, have measured defect concentrations that are zero within analytical uncertainty (see Table 2). Thus, although the actual final "quench" f_{O_2} and temperature conditions are unknown, spinels equilibrated at 1400°C and 10^{-4} atm are essentially stoichiometric.

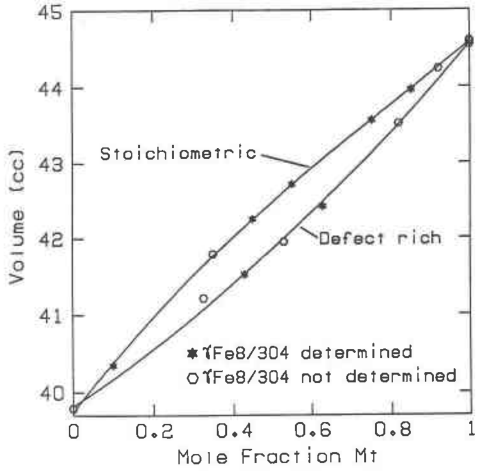

Fig. 2 Molar volumes of defect-rich compared with stoichiometric spinels across the $MgAl_2O_4$-Fe_3O_4 join. Stoichiometric data are the same as those plotted in Fig. 1. Data labeled defect-rich are for spinels re-equilibrated at 1000°C and "oxidized" f_{O_2} (see Table 1 and text for discussion). As in Fig. 1, the lines are least-squares fits to the plotted data. Symbols are the same as in Fig. 1.

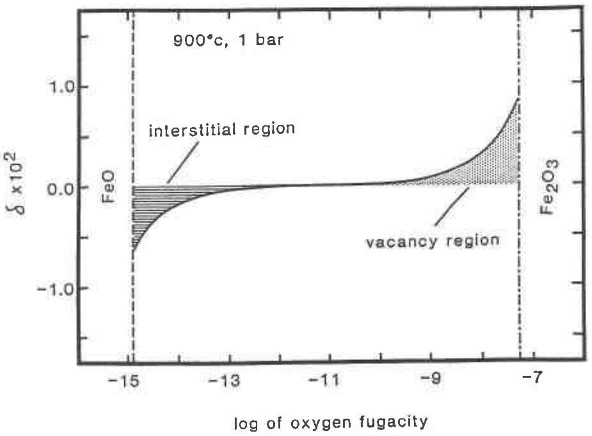

Fig. 3. The stoichiometry parameter, δ, for $Fe_{3-\delta}O_4$ at 900°C as a function of f_{O_2} (Dieckmann, 1982). The vertical dashed line corresponds to the Fe_3O_4 phase boundary with $Fe_{1-\Delta}O$, whereas the dot-dashed line corresponds to the Fe_3O_4 phase boundary with $Fe_{2+\epsilon}O_3$. The lined area indicates the f_{O_2} region in which interstitial Fe^{2+} is the dominant equilibrium defect in Fe_3O_4. The dotted area indicates the f_{O_2} region in which octahedral vacancies predominate as the equilibrium defect species.

The air and 10^{-4} atm f_{O_2} syntheses are both fit best by cubic polynomials, yielding asymmetric terms for excess volume of mixing (see preceding discussion). As with the 1.0% CO and "oxidized" samples from 1000°C, the spinels with the highest $\gamma Fe_{8/3}O_4$ concentrations, in this case, those synthesized in air, have the smallest cell edges. The differences in cell edge and molar volume between the air and 10^{-4} atm data also increase with increasing Fe_3O_4 content and persist across the entire $MgAl_2O_4$-Fe_3O_4 join (see Fig. 1). The concentration of $\gamma Fe_{8/3}O_4$ does not, however, continue to increase across the join with increasing Fe_3O_4 concentration. There are several possible explanations for this phenomenon: (1) the wet-chemical data may be too imprecise to record the true $\gamma Fe_{8/3}O_4$ concen-

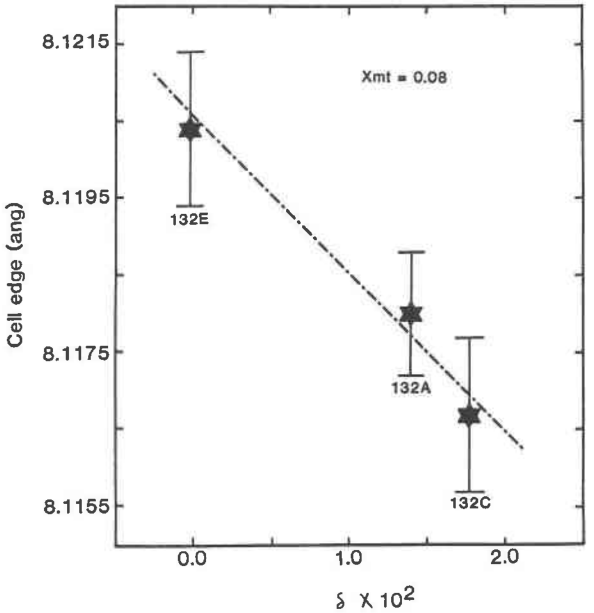

Fig. 4. Cell edge vs. δ for three synthetic spinels with nominal $X_{Fe_3O_4}$ equal to 0.08 (see Table 2). Error bars represent $\pm 1\sigma$ for cell-edge determinations. The dot-dash line is not the result of a least-squares fit; however, it does show the very nearly linear inverse relation of cell edge with δ for spinels of low $X_{Fe_3O_4}$.

tration; (2) the defect population may continue to equilibrate with the ambient atmosphere, whereas the cell edge remains insensitive to further change after some critical defect concentration; or (3) there may be ternary excess-volume effects within the system, which are not explained by simple extrapolation of the binary data into the complex ternary volume space, as discussed more extensively below.

All of the $MgAl_2O_4$-Fe_3O_4 cell-edge data indicate that the presence of $\gamma Fe_{8/3}O_4$ component in spinel decreases the cell edge and hence molar volume, at constant Fe_3O_4 concentration. This is in agreement with data on cell edge and molar volume along the join Fe_3O_4-γFe_2O_3 (Lindsley, 1976). We have corrected the apparent excess-volume fit to the Fe_3O_4-γFe_2O_3 molar volumes presented by Lindsley to a four-oxygen basis ($\gamma Fe_{8/3}O_4$) for direct comparison with the current syntheses along the $MgAl_2O_4$-Fe_3O_4 join. When this is done, volume of mixing between Fe_3O_4 and $\gamma Fe_{8/3}O_4$ is essentially linear and thus is consistent with current observations. The corrected Fe_3O_4-$\gamma Fe_{8/3}O_4$ cell-edge data are plotted in Figure 5.

THERMODYNAMIC MODEL

Thermodynamic state functions are often modeled as linear combinations of so-called "ideal" and "excess" terms. In the foregoing discussion, we presented experimental data and derived excess parameters for one of the three bounding binary joins, $MgAl_2O_4$-Fe_3O_4, of the $MgAl_2O_4$-Fe_3O_4-$\gamma Fe_{8/3}O_4$ ternary-spinel system. Our fit to one of the other two bounding joins, Fe_3O_4-$\gamma Fe_{8/3}O_4$, suggests that there is no excess volume of mixing across this join. Using these constraints, we may now describe cell edges in the nonideal $MgAl_2O_4$-Fe_3O_4-$\gamma Fe_{8/3}O_4$ ternary system.

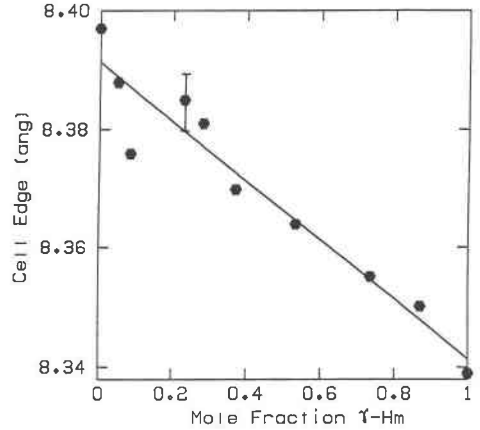

Fig. 5. Cell edge vs. $X_{\gamma Fe_{8/3}O_4}$ for the Fe_3O_4-$\gamma Fe_{8/3}O_4$ spinel join. Data shown as filled hexagons are those presented by Lindsley (1976). The size of the symbols is approximately equal to our estimate of $\pm 1\sigma$. One datum is plotted with an explicit error bar corresponding to $\pm 1\sigma$, as presented by Lindsley (1976). Note the essentially ideal cell edge–composition relation for this bounding binary of the $MgAl_2O_4$-Fe_3O_4-$\gamma Fe_{8/3}O_4$ ternary-spinel system.

A valid Margules formulation for an asymmetric ternary solution has recently been presented by Andersen and Lindsley (1981). They obtained a general equation for a ternary solution of the form

$$\begin{aligned} V^{xs} = {} & W_{12}(X_1X_2)(X_2 + \tfrac{1}{2}X_3) \\ & + W_{21}(X_1X_2)(X_1 + \tfrac{1}{2}X_3) \\ & + W_{13}(X_1X_3)(X_3 + \tfrac{1}{2}X_2) \\ & + W_{31}(X_1X_3)(X_1 + \tfrac{1}{2}X_2) \\ & + W_{23}(X_2X_3)(X_3 + \tfrac{1}{2}X_1) \\ & + W_{32}(X_2X_3)(X_2 + \tfrac{1}{2}X_1) \\ & + W_{123}(X_1X_2X_3), \end{aligned} \tag{3}$$

where W_{12}, W_{21}, etc., are the binary asymmetric Margules parameters, X_1 is the mole fraction of component 1, in this case, Fe_3O_4 (component 2 = $MgAl_2O_4$, and component 3 = $\gamma Fe_{8/3}O_4$), and W_{123} is the ternary interaction parameter. The ideal contribution to the ternary molar volume

TABLE 6. $MgAl_2O_4$-Fe_3O_4-$\gamma Fe_{8/3}O_4$ ternary fit parameters

	Order of ternary model		
	(0)	(1)	(2)
N:	14	14	14
W_{23} (cal/bar)	0.013(0.061)	−0.079(0.311)	−0.162(0.370)
W_{32} (cal/bar)	0.013(0.061)	0.056(0.158)	0.036(0.170)
W_{123} (cal/bar)	—	—	0.348(0.773)
F_x*	—	0.14	0.35

Note: Values in parentheses are $\pm 1\sigma$.

* F_x values indicate that models of order (1) and (2) are not statistically significant.

is expressed as a weighted average of the end-member volumes, as follows:

$$V^{\mathrm{id}} = V_1^0 X_1 + V_2^0 X_2 + V_3^0 X_3. \tag{4}$$

Equation 3 may be simplified by substituting our derived Margules parameters for $MgAl_2O_4$-Fe_3O_4, $W^V_{\mathrm{mt\text{-}sp}}$ and $W^V_{\mathrm{sp\text{-}mt}}$ and by letting $W^V_{\mathrm{mt\text{-}\gamma hm}} = W^V_{\mathrm{\gamma hm\text{-}mt}} = 0.0$ cal/bar. An iterative, nonlinear least-squares numerical method was used to determine the ternary fit parameters. Excluding the 13 stoichiometric spinels synthesized at 1400°C and 10^{-4} atm that were used to constrain the volume relations across the $MgAl_2O_4$-Fe_3O_4 binary, 14 ternary-spinel solutions, with known X_1, X_2, and X_3 concentrations and molar volumes, were used to obtain values for W_{23}, W_{32}, and W_{123}. The ternary fit coefficients, their associated standard errors, and corresponding F values are presented in Table 6.

The ternary volumes are fit best by a single symmetric Margules parameter for the $MgAl_2O_4$-$\gamma Fe_{8/3}O_4$ join ($W_{23} = W_{32} = 0.013 \pm 0.061$); unfortunately, the volume-composition data are not precise enough to determine whether the $MgAl_2O_4$-$\gamma Fe_{8/3}O_4$ join is asymmetric at the 95% confidence level or whether a ternary-interaction parameter is required. Moreover, the derived symmetric Margules parameter for the $MgAl_2O_4$-$\gamma Fe_{8/3}O_4$ join, W_{23}, has a standard error nearly five times as large as the best-fit value (see Table 6) and thus is poorly constrained by the current data. Accordingly, we have set W_{23} equal to 0.0 for all further calculations. An ideal volume-of-mixing model for the $MgAl_2O_4$-$\gamma Fe_{8/3}O_4$ join, moreover, is consistent with experimental results for the analogous defect aluminate spinel join, $MgAl_2O_4$-$\gamma Al_{8/3}O_4$, along which volume and enthalpy of mixing are both essentially ideal (Navrotsky et al., 1986).

The model for ternary-spinel volumes is expressed as the sum of Equations 3 and 4. Making the appropriate substitutions and including only nonzero Margules parameters, we obtain

$$\begin{aligned} V^{\mathrm{ss}} = {} & V_1^0 X_1 + V_2^0 X_2 + V_3^0 X_3 \\ & + W_{12}(X_1X_2)(X_2 + \tfrac{1}{2}X_3) \\ & + W_{21}(X_1X_2)(X_1 + \tfrac{1}{2}X_3). \end{aligned} \tag{5}$$

Equation 5 must then be differentiated with respect to X_1, X_2, and X_3 to obtain $\bar{V}_1$, $\bar{V}_2$, and $\bar{V}_3$, respectively. This results in the following expressions:

$$\begin{aligned} \bar{V}_1 = {} & V_1^0 + W_{12}(X_2^2 - 2X_1X_2^2 + \tfrac{1}{2}X_2X_3 - X_1X_2X_3) \\ & + W_{21}(2X_1X_2^2 + \tfrac{1}{2}X_2X_3 + X_1X_2X_3) \end{aligned} \tag{6}$$

$$\begin{aligned} \bar{V}_2 = {} & V_2^0 + W_{12}(2X_1^2X_2 + \tfrac{1}{2}X_1X_3 + X_1X_2X_3) \\ & + W_{21}(X_1^2 - 2X_1^2X_2 + \tfrac{1}{2}X_1X_3 - X_1X_2X_3) \end{aligned} \tag{7}$$

$$\begin{aligned} \bar{V}_3 = {} & V_3^0 + W_{12}(X_1^2X_2 - X_1X_2^2 - \tfrac{1}{2}X_1X_2) \\ & + W_{21}(X_1X_2^2 - X_1^2X_2 - \tfrac{1}{2}X_1X_2), \end{aligned} \tag{8}$$

where $\bar{V}_1 = \bar{V}_{\mathrm{mt}}$, $\bar{V}_2 = \bar{V}_{\mathrm{sp}}$, $\bar{V}_3 = \bar{V}_{\mathrm{\gamma hm}}$, $V_1^0 = V_{\mathrm{mt}}^0 = 1.066 \pm 0.014$, $V_2^0 = V_{\mathrm{sp}}^0 = 0.950 \pm 0.001$, $V_3^0 = V_{\mathrm{\gamma hm}}^0 = 1.043 \pm 0.018$, $W_{12} = W^V_{\mathrm{mt\text{-}sp}} = 0.043 \pm 0.012$ cal/bar, and $W_{21} = W^V_{\mathrm{sp\text{-}mt}} = 0.018 \pm 0.004$ cal/bar. Equations 6, 7, and 8 completely characterize partial molar volumes in the $MgAl_2O_4$-Fe_3O_4-$\gamma Fe_{8/3}O_4$ ternary-spinel system. These expressions may be used to estimate the effect of pressure on intrinsic f_{O_2} measurements of spinel separates from mantle-derived xenoliths entrained in alkalic magmas. In addition, $\bar{V}_{\mathrm{mt}}$ may be used to correct polyphase thermobarometric f_{O_2} estimates for spinel lherzolites to their appropriate equilibrium pressure. Results of these calculations are discussed further below.

COMPARISON WITH THE O'NEILL AND NAVROTSKY MODEL

Cation distribution

There have been many attempts to model the thermodynamics for the cation distribution of spinels (Kriessman and Harrison, 1956; Dunitz and Orgel, 1957; McClure, 1957; Navrotsky and Kleppa, 1967; Navrotsky, 1969; Glidewell, 1976; Urusov, 1981, 1983; O'Neill and Navrotsky, 1983, 1984), and these models may, in principle, be used to extrapolate outside the temperature, pressure, and composition region covered by experimental data. The recent efforts of O'Neill and Navrotsky (1983, 1984) provide a rational framework in which to analyze a variety of thermodynamic data now available for end-member and complex binary spinels. Their model was formulated on the basis of lattice-energy arguments, which suggest that the electrostatic contribution to the total internal energy of a spinel phase is several orders of magnitude greater than either the repulsive or vibrational contributions. Both the electrostatic and repulsive contributions have, however, a quadratic dependence on the degree of internal disorder or inversion, χ. O'Neill and Navrotsky have suggested further that if the PV term for the total internal energy is ignored, then the enthalpy of disordering (in kcal/mol) has the same quadratic form as the electrostatic and repulsive lattice energies and may be written as

$$\Delta H_{\mathrm{D}} = \alpha\chi + \beta\chi^2, \tag{9}$$

where α and β are empirical constants, which have units of energy.

We have applied the O'Neill and Navrotsky formalism to the $MgAl_2O_4$-Fe_3O_4 spinel join, in order to ascertain whether their model is able to explain our observed molar-volume data. The complete results of these calculations and the details of the numerical methods used to solve for the equilibrium cation distribution as a function of temperature and composition along the join $MgAl_2O_4$-Fe_3O_4 are presented elsewhere (Mattioli and Wood, 1987). The relevant cation-disordering equilibria are as follows:

$$\begin{aligned} Fe^{2+} + (Fe^{3+}) &= (Fe^{2+}) + Fe^{3+} \\ \Delta H_{\mathrm{D}} &= 7.76\chi - 6.15\chi^2 \end{aligned} \tag{10}$$

$$\begin{aligned} Fe^{2+} + (Al^{3+}) &= (Fe^{2+}) + Al^{3+} \\ \Delta H_{\mathrm{D}} &= 14.20\chi - 7.24\chi^2 \end{aligned} \tag{11}$$

$$\begin{aligned} Mg^{2+} + (Al^{3+}) &= (Mg^{2+}) + Al^{3+} \\ \Delta H_{\mathrm{D}} &= 9.84\chi - 6.63\chi^2 \end{aligned} \tag{12}$$

$$\begin{aligned} Mg^{2+} + (Fe^{3+}) &= (Mg^{2+}) + Fe^{3+} \\ \Delta H_{\mathrm{D}} &= 3.40\chi - 5.54\chi^2 \end{aligned} \tag{13}$$

where the species in parentheses reside on the octahedral site, χ is the degree of inversion (a dimensionless parameter), and ΔH_D is the enthalpy of disordering in kcal/mol. Only three of the four possible cation-disordering equilibria are linearly independent (i.e., Eq. 13 = Eq. 10 + Eq. 12 − Eq. 11). The values of α and β for equilibria 10 and 11 used for our calculations were taken from experimental data of Wu and Mason (1981) and Mason (1985), respectively. Results for Equation 12 were extracted from ^{27}Al NMR spectroscopic data on pure $MgAl_2O_4$ spinels drop-quenched to 25°C in H_2O from 700 to 1000°C (Wood et al., 1986). Transposed-temperature-drop calorimetry also has been applied recently to determine ΔH_D for $MgAl_2O_4$ and $MgFe_2O_4$ (Eqs. 12 and 13) (Navrotsky, 1986). The enthalpy data are in good agreement with the parameters used in our calculations. Our derived α and β values for equilibrium 13, moreover, are in good agreement with high-temperature thermopower measurements (Trestman-Matts et al., 1984), if an experimental uncertainty of ±1 kcal in the latter is assumed. This indicates that all experimental data for the equilibria of interest have reasonable internal consistency. The values of α and β presented above were used to determine equilibrium cation distributions at $0.01X_{mt}$ intervals between 500 and 1400°C at intervals of every 100 deg.

The derived cation distribution at each composition and temperature was used to calculate the cell edge and oxygen parameter across the $MgAl_2O_4$-Fe_3O_4 spinel join. We used the optimized cation radii of O'Neill and Navrotsky (1983), which they revised from the larger data set of Shannon and Prewitt (1969) and Shannon (1976). The oxygen radius was fixed at 1.38 Å for both tetrahedral and octahedral coordination. As suggested by Hill et al. (1979), tetrahedral- and octahedral-site radii were then calculated as a sum of the cation radii multiplied by the cation-site fractions. If the sums of the tetrahedral and octahedral radii are known and we define R as the ratio of R_{oct} to R_{tet}, then the oxygen parameter, u, may be calculated from the following equation of Hill et al. (1979):

$$u = \frac{(R^2/4) - (2/3) + [(11R^2/48) - (1/18)]^{1/2}}{2R^2 - 2}. \qquad (14)$$

From tetrahedral and octahedral radii, cell edges are then given by the following expressions:

$$a_{tet} = \frac{R_{tet}}{\sqrt{3}[u - (1/8)]} \qquad (15)$$

$$a_{oct} = \frac{R_{oct}}{[3u^2 - 2u + (3/8)]^{1/2}}. \qquad (16)$$

Tetrahedral and octahedral cell edges calculated in this way are always equal. The model cell edge–composition relations at 500, 1000, and 1400°C, together with the stoichiometric spinel data quenched from 1400°C and f_{O_2} of 10^{-4} atm, are presented in Figure 6.

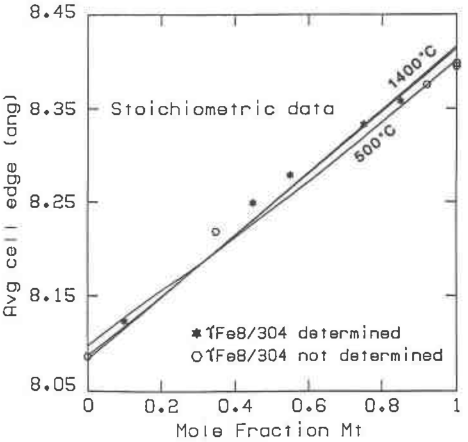

Fig. 6. Comparison of our stoichiometric-spinel cell edges across the $MgAl_2O_4$-Fe_3O_4 join with cell edges calculated using the O'Neill and Navrotsky (1983, 1984) cation-distribution model at 500, 1000 (not labeled), and 1400°C. Note the poor agreement of predicted cell edges with observed cell edges "quenched" from 1400°C.

Calculated cell edge–composition relations (Fig. 6) change as a function of temperature, but the sign and magnitude of the predicted excess volumes are in poor agreement with observed volumes for stoichiometric spinels on the $MgAl_2O_4$-Fe_3O_4 join. As temperature is increased from 500 to 1400°C, the model predicts that excess volume decreases nearly to zero, in contrast to our observed positive excess volume for complex spinels quenched from both 1000 and 1400°C.

Although the O'Neill and Navrotsky model reproduces the observed cation distributions in the end members $MgAl_2O_4$ and Fe_3O_4, calculated cation distributions for complex spinels may be in error because of short-range order. Previous studies of pure $MgAl_2O_4$ and $MgAl_2O_4$-$\gamma Al_{8/3}O_4$ solid solutions suggest that short-range order is significant for spinels containing an $MgAl_2O_4$ component (Wood et al., 1986; Navrotsky et al., 1986). Such effects are not explicitly incorporated into our current formulation of $MgAl_2O_4$-Fe_3O_4 cation disorder. In addition to short-range order, the effect of different rates of equilibration for the internal cation-disordering equilibria (Eqs. 10–13) may further complicate the application of the O'Neill-Navrotsky model to spinels quenched from high temperature. Comparison of our measured end-member cell-edge data with those calculated from the model suggests that the $MgAl_2O_4$ component had its equilibrium cation distribution set at a higher temperature than the Fe_3O_4 component (see Fig. 6). The equilibrium cation distribution at about 1000°C yields a predicted cell edge for pure $MgAl_2O_4$ (at 25°C) that is in agreement with the observed cell edge for $MgAl_2O_4$ quenched from high temperature. In contrast, the observed and predicted cell edges for pure Fe_3O_4 are in agreement when the equilibrium cation distribution is calculated at about 400°C. These results are not surprising since Mg-Al disorder requires physical displacement of cations between tetrahedral and octahedral sublattices, whereas Fe^{2+}-Fe^{3+} disorder only

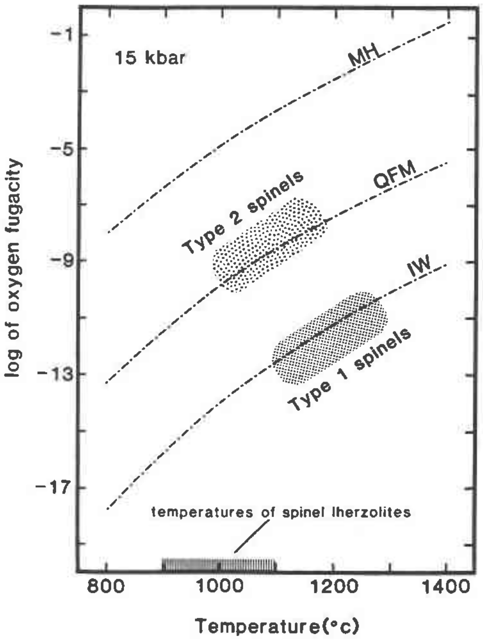

Fig. 7. Published intrinsic f_{O_2} values of mantle spinels from Arculus and Delano (1981) and Arculus et al. (1984) corrected to 15-kbar total pressure using our ternary-spinel volume model. The pressure-corrected synthetic Fe-bearing buffers as well as the approximate temperatures recorded by spinel lherzolite xenoliths are shown for reference. Note that 15-kbar total pressure does not significantly increase the intrinsic f_{O_2} values of type 1 spinels above IW.

entails transfer of an electron between sublattices. A more complete test of the O'Neill-Navrotsky model, as applied to this system, would require determinations of cell edges and cation distributions at high temperature.

Petrologic application

Intrinsic f_{O_2} measurements

It has been suggested that the 1-atm intrinsic f_{O_2} measurements of mantle spinels record an f_{O_2} that may need to be corrected to their actual equilibration pressures in the mantle (Arculus and Delano, 1981; Arculus et al., 1984). We may use our derived values of $\bar{V}_{mt}$ and $\bar{V}_{\gamma hm}$ to estimate the effect of pressure on published intrinsic f_{O_2} measurements of spinel separates from mantle-derived spinel lherzolite xenoliths (Arculus and Delano, 1980, 1981; Arculus et al., 1984). Homogeneous internal defect equilibria for Fe^{2+}, Fe^{3+}, V_{oct}, and Fe^{2+}_{int} define the intrinsic f_{O_2} of any spinel phase (Dieckmann, 1982). These defect equilibria may be simplified to an oxidation-reduction equilibrium involving Fe_3O_4 and $\gamma Fe_{8/3}O_4$ components in the spinel phase, as follows:

$$4.5\gamma Fe_{8/3}O_4 \text{ (in spinel)} = 4Fe_3O_4 \text{ (in spinel)} + O_2. \quad (17)$$

The maximum effect of pressure on equilibrium 17 may be calculated using $\bar{V}_{mt}$ and $\bar{V}_{\gamma hm}$ derived above, if we assume infinite dilution (i.e., $X_{mt} = X_{\gamma hm} = 0.0$ and $X_{sp} = 1.0$) at some constant temperature. Under these conditions, Equations 6 and 8 reduce to the following expressions:

$$\bar{V}_1 = V_1^0 + W_{12} \quad (18)$$
$$\bar{V}_3 = V_3^0, \quad (19)$$

where $\bar{V}_1 = \bar{V}_{mt}$, $\bar{V}_3 = \bar{V}_{\gamma hm}$, and $W_{12} = W^V_{mt\text{-}sp} = 0.043 \pm 0.012$ cal/bar. The equation governing f_{O_2} at a given temperature and pressure is

$$\log f_{O_2}^{T,P} = \log f_{O_2}^{T,1\text{ atm}} - \frac{1}{2.303RT}\int_1^P \Delta\bar{V}_r\, dP', \quad (20)$$

where R is the universal gas constant, T is temperature in K, and $\Delta\bar{V}_r$ is in cal/bar. If we assume that the change in partial molar volume for equilibrium 17, $\Delta\bar{V}_r$, is independent of temperature and pressure, then Equation 20 may be integrated to evaluate the effect of pressure on intrinsic f_{O_2}.

Applying the conditions stated above and ignoring the small effects of isobaric expansion and isothermal compression, we find that $\Delta\bar{V}_{17}$ is equal to -0.258 cal/bar. Assuming a temperature of 1000°C, the calculated increase in intrinsic f_{O_2} is $+0.66$ log units at 15 kbar and $+1.33$ log units at 30 kbar. Relative to the synthetic QFM buffer, however, $\Delta(\log f^P_{O_2}\text{(intrinsic)} - \log f^P_{O_2}\text{(buffer)})$ equals -0.47 log units at 15 kbar and -0.94 log units at 30 kbar. In contrast, relative to the IW buffer, the difference is equal to $+0.06$ log units at 15 kbar and $+0.12$ log units at 30 kbar. The published intrinsic measurements of mantle spinels, corrected to 15-kbar total pressure, are presented in Figure 7. These calculations clearly demonstrate that high pressures do not significantly alter the measured 1-atm intrinsic f_{O_2} values relative to the synthetic Fe-bearing buffers (Mattioli and Wood, 1985). Other factors, such as C interference or autoreduction (Moats et al., 1986), must play more important roles in producing the apparently low intrinsic f_{O_2} values reported by Arculus and Delano (1980, 1981) and Arculus et al. (1984).

Thermobarometric f_{O_2} calculations

The equilibrium f_{O_2} for spinel lherzolite xenoliths may also be calculated from heterogeneous equilibria, such as

$$2Fe_3O_4 \text{ (in spinel)} + 6FeSiO_3 \text{ (in orthopyroxene)} = 6Fe_2SiO_4 \text{ (in olivine)} + O_2. \quad (21)$$

If standard-state (Bohlen et al., 1980; Myers and Eugster, 1983), activity-composition (Wood and Kleppa, 1981), and electron-microprobe or some other mineral-composition data are available (see, e.g., Frey and Prinz, 1978), then an f_{O_2} for the three-phase assemblage (spinel-orthopyroxene-olivine) may be calculated directly from equilibrium 21. Mattioli and Wood (1986a, 1987) used experimentally calibrated Fe_3O_4 activity in $MgAl_2O_4$-rich spinel to estimate f_{O_2} in the spinel lherzolite facies of the Earth's upper mantle. Their results indicate that upper-mantle f_{O_2} is heterogeneous, although generally within ±2 log units of QFM. The current volume data may be used to correct natural xenolith data to the appropriate equilibrium pressure. Data on partial molar volumes for ferrosilite and fayalite were taken from Newton and Wood (1980) and Fisher and Medaris (1967), respectively. If we fix $X^{opx}_{fs} = X^{ol}_{fa} = 0.10$, $X^{sp}_{mt} = 0.01$ and ignore the small effects of isobaric expansion and isothermal compression on the phases, then $\Delta\bar{V}_{21} = -0.228$ cal/bar. At 1000°C, this corresponds to an absolute increase in f_{O_2} relative to 1-atm pressure of +0.59 log units at 15 kbar and +1.17 log units at 30 kbar. Relative to QFM, this corresponds to a change in f_{O_2} of −0.74 log units at 15 kbar and −1.12 log units at 30 kbar. The effect of pressure on equilibrium 21 therefore is quite small, which implies that compositional variation plays a more important role in controlling upper-mantle f_{O_2} heterogeneity.

CONCLUSIONS

Cell edges and molar volumes of $MgAl_2O_4$-Fe_3O_4 pseudobinary spinels are decreased by small concentrations of $\gamma Fe_{8/3}O_4$ spinel component. We have fit the three bounding binary joins of the $MgAl_2O_4$-Fe_3O_4-$\gamma Fe_{8/3}O_4$ ternary-spinel system by least-squares regression and found that both the Fe_3O_4-$\gamma Fe_{8/3}O_4$ and the $MgAl_2O_4$-$\gamma Fe_{8/3}O_4$ binaries show ideal volumes of mixing within experimental uncertainty. The $MgAl_2O_4$-Fe_3O_4 binary, however, is fit at the 95% confidence level by an asymmetric Margules formulation. These data constrain partial molar volumes in the ternary-spinel system and thus may be used to calculate the effect of pressure on both intrinsic and thermobarometric f_{O_2}. In both cases, the effects of pressures up to 30 kbar are small (about 1 log unit). At this time, the apparently low f_{O_2} values recorded by some intrinsic measurements cannot be reconciled with thermobarometric f_{O_2} estimates for spinels with similar X_{mt} concentrations (Mattioli and Wood, 1986a, 1987).

The observed cell-edge data for the $MgAl_2O_4$-Fe_3O_4 join were compared to predicted cell edges based on cation distributions calculated between 500 and 1400°C using the O'Neill and Navrotsky (1983, 1984) model. We have found that their model does not predict correct cell edge–composition relations along this join, probably because of different equilibration rates among the three internal cation-disordering equilibria (Eqs. 10–12) and an unknown amount of short-range order. Controlled f_{O_2} experiments with in situ structural refinements and thermopower determinations of cation distributions would greatly improve our understanding of order-disorder relations in complex binary spinels.

ACKNOWLEDGMENTS

This research was supported in part by NSF Grants EAR-821502 and EAR-8409666 to B.J.W. G.S.M. would like to thank Craig Bina and Phillip Bryan for helpful discussions on numerical methods used to solve partial differential equations. George Helffrich is thanked for providing the software used to calculate the ternary fit parameters. We also thank Roger Powell and Alexandra Navrotsky for their careful reviews of this manuscript.

REFERENCES

Albee, A.L., and Ray, L. (1970) Correction factors for electron probe microanalysis of silicates, oxides, carbonates, phosphates, and sulfates. Analytical Chemistry, 42, 1408–1414.

Andersen, D.J., and Lindsley, D.H. (1981) A valid Margules formulation for an asymmetric ternary solution: Revision of the olivine-ilmenite thermometer, with applications. Geochimica et Cosmochimica Acta, 45, 847–853.

Arculus, R.J., and Delano, J.W. (1980) Implications for the primitive atmosphere of the oxidation state of Earth's upper mantle. Nature, 288, 72–74.

——— (1981) Intrinsic oxygen fugacity measurements: Techniques and results for spinels from upper mantel peridotites and megacryst assemblages. Geochimica et Cosmochimica Acta, 45, 899–913.

Arculus, R.J., Dawson, J.B., Mitchell, R.H., Gust, D.A., and Holmes, R.D. (1984) Oxidation states of the upper mantle recorded by megacryst ilmenite in kimberlite and type A and B spinel lherzolites. Contributions to Mineralogy and Petrology, 85, 85–94.

Bence, A.E., and Albee, A.L. (1968) Empirical correction factors for the electron microanalysis of silicates and oxides. Journal of Geology, 6, 382–403.

Bevington, P.R. (1969) Data reduction and error analysis for the physical sciences. McGraw-Hill, New York, 336 p.

Bohlen, S.R., Essene, E.J., and Boettcher, A.L. (1980) Reinvestigation and application of olivine-quartz-orthopyroxene barometry. Earth and Planetary Science Letters, 47, 1–10.

Buddington, A.F., and Lindsley, D.H. (1964) Iron-titanium oxide minerals and their synthetic equivalents. Journal of Petrology, 35, 310–357.

Deines, P., Nafziger, R.H., Ulmer, G.C., and Woermann, E. (1974) Temperature–oxygen fugacity tables for selected gas mixtures in the system C-H-O at one atmosphere total pressure. Pennsylvania State University, College of Earth and Mineral Sciences, Bulletin of the Experiment Station, 88, 129 p.

Dieckmann, R. (1982) Defects and cation diffusion in magnetite (IV): Nonstoichiometry and point defect structure of magnetite ($Fe_{3-\delta}O_4$). Berichte Bunsengesellschaft Physikalische Chemie, 86, 112–118.

Dieckmann, R., and Schmalzried, H. (1982) Defects and cation diffusion in magnetite (II). Berichte Bunsengesellschaft Physikalische Chemie, 81, 414–419.

Dunitz, J.D., and Orgel, L.E. (1957) Electronic properties of transition-metal oxides-II. Physics and Chemistry of Solids, 3, 318–323.

Fisher, G.W., and Medaris, L.G. Jr. (1969) Cell dimensions and X-ray determinative curve for synthetic Mg-Fe olivines. American Mineralogist, 54, 741–753.

Frey, F.A., and Prinz, M. (1978) Ultramafic inclusions from San Carlos, Arizona: Petrologic and geochemical data bearing on their petrogenesis. Earth and Planetary Science Letters, 38, 129–176.

Gasparik, T., and Newton, R.C. (1984) The reversed alumina contents of orthopyroxene in equilibrium with spinel and forsterite in the system MgO-Al_2O_3-SiO_2. Contributions to Mineralogy and Petrology, 85, 186–196.

Glidewell, C. (1976) Cation distribution in spinels: Lattice energy versus crystal field stabilisation energy. Inorganica Chimica Acta, 19, L45–47.

Hill, R.L., and Sack, R.O. (1987) Thermodynamic properties of Fe-Mg titanomagnetite spinels. Canadian Mineralogist, in press.

Hill, R.J., Craig, J.R., and Gibbs, G.V. (1979) Systematics of the spinel structure type. Physics and Chemistry of Minerals, 4, 317–339.

Kriessman, C.J., and Harrison, S.E. (1956) Cation distributions in ferrospinels; magnesium-manganese ferrites. American Ceramic Society Journal, 103, 857–860.

Lindsley, D.H. (1976) The crystal chemistry and structure of oxide minerals as exemplified by the Fe-Ti oxides. Mineralogical Society of America Reviews in Mineralogy, 3, L1–60.

Mason, T.O. (1985) High-temperature cation distributions in Fe_3O_4-$FeAl_2O_4$. American Ceramic Society Journal, 68, C74–75.

Mattioli, G.S., and Wood, B.J. (1985) Activities and volumes in $MgAl_2O_4$-Fe_3O_4-$\gamma Fe_{8/3}O_4$ spinels: Implications for mantle oxygen fugacity. Geological Society of America Abstracts with Programs, 17, 655.

——— (1986a) Upper mantle oxygen fugacity recorded by spinel-lherzolites. Nature, 322, 626–628.

——— (1986b) Experimental determination of Fe_3O_4 activity in complex spinels: Implications for upper mantle f_{O_2}. International Mineralogical Association Abstracts with Program, 14, 168.

——— (1987) Magnetite activities across the $MgAl_2O_4$-Fe_3O_4 spinel join, with application to thermobarometric estimates of upper mantle oxygen fugacity. Contributions to Mineralogy and Petrology, in press.

McClure, D.S. (1957) The distribution of transition metal cations in spinels. Physics and Chemistry of Solids, 3, 311–317.

Moats, M.A., Ulmer, G.C., and Virgo, D. (1986) Interpreting IOF results for ilmenite-bearing xenoliths using Mössbauer spectrometry. EOS, 67, 414.

Myers, J., and Eugster, H.P. (1983) The system Fe-Si-O: Oxygen buffer calibrations to 1,500K. Contributions to Mineralogy and Petrology, 82, 75–90.

Navrotsky, A. (1969) Thermodynamics of A_3O_4-B_3O_4 solid solutions. Journal of Inorganic and Nuclear Chemistry, 31, 59–72.

——— (1986) Cation-distribution energetics and heats of mixing in $MgFe_2O_4$-$MgAl_2O_4$, $ZnFe_2O_4$-$ZnAl_2O_4$, and $NiAl_2O_4$-$ZnAl_2O_4$ spinels: Study by high temperature calorimetry. American Mineralogist, 71, 1160–1169.

Navrotsky, A., and Kleppa, O.J. (1967) The thermodynamics of formation of simple spinels. Journal of Inorganic and Nuclear Chemistry, 30, 479–498.

Navrotsky, A., Wechsler, B.A., Geisinger, K., and Seifert, F. (1986) Thermochemistry of $MgAl_2O_4$-$\gamma Al_{8/3}O_4$ defect spinels. American Ceramic Society Journal, 69, 418–422.

Newton, R.C., and Wood, B.J. (1980) Volume behavior of silicate solid solutions. American Mineralogist, 65, 733–745.

O'Neill, H.St.C., and Navrotsky, A. (1983) Simple spinels: Crystallographic parameters, cation radii, lattice energies, and cation distribution. American Mineralogist, 68, 181–194.

——— (1984) Cation distributions and thermodynamic properties of binary spinel solutions. American Mineralogist, 69, 733–753.

Powell, R. (1985) Regression diagnostics and robust regression in geothermometer/geobarometer calibration: The garnet-clinopyroxene geothermometer revisited. Journal of Metamorphic Geology, 8, 231–243.

Sack, R.O. (1982) Spinels as petrologic indicators: Activity-composition relations at low pressures. Contributions to Mineralogy and Petrology, 79, 169–186.

Sato, M. (1971) Electrochemical measurements and control of oxygen fugacity and other gaseous fugacities with solid electrolyte systems. In G.C. Ulmer, Ed., Research techniques for high pressure and high temperature, p. 43–100. Springer-Verlag, New York.

Shannon, R.D. (1976) Revised effective ionic radii and systematic studies of interatomic distances in halides and chalcogenides. Acta Crystallographica, A32, 751–767.

Shannon, R.D., and Prewitt, C.T. (1969) Effective ionic radii in oxides and fluorides. Acta Crystallographica, B25, 925–946.

Trestman-Matts, A., Dorris, S.E., Kumarakrishnan, S., and Mason, T.O. (1983) Thermoelectric determination of cation distributions in Fe_3O_4-Fe_2TiO_4. American Ceramic Society Journal, 66, 829–834.

Trestman-Matts, A., Dorris, S.E., and Mason, T.O. (1984) Thermoelectric determination of cation distributions in Fe_3O_4-$MgFe_2O_4$. American Ceramic Society Journal, 67, 69–74.

Urusov, V.S. (1981) Cation distributions in spinels: Effective electrostatic energy versus crystal field stabilization energy. Crystal Research and Technology, 16, K62–64.

——— (1983) Interaction of cations on octahedral and tetrahedral sites in simple spinels. Physics and Chemistry of Minerals, 9, 1–5.

Wilson, A.D. (1960) The micro-determination of ferrous iron in silicate minerals by a volumetric and colorimetric method. Analyst, 85, 823–827.

Wood, B.J., and Kleppa, O.J. (1981) Thermochemistry of fosterite-fayalite olivine solutions. Geochimica et Cosmochimica Acta, 45, 529–534.

Wood, B.J., Kirkpatrick, R.J., and Montez, B. (1986) Order-disorder phenomena in $MgAl_2O_4$ spinel. American Mineralogist, 71, 999–1006.

Wu, C.C., and Mason, T.O. (1981) Thermopower measurement of cation distribution in magnetite. American Ceramic Society Journal, 64, 520–522.

MANUSCRIPT RECEIVED JULY 30, 1986
MANUSCRIPT ACCEPTED JANUARY 30, 1987